MM-Wave Tapered Slot Antennas on Synthesized Low Permittivity Substrates

Jeremy B. Muldavin and Gabriel M. Rebeiz
Radiation Laboratory, Department of Electrical Engineering and Computer Science,
University of Michigan, Ann Arbor, Michigan, 48109-2122, USA.
muldavin@engin.umich.edu, rebeiz@umich.edu.

Abstract— **This paper presents 30 GHz linear tapered slot antennas (LTSA) and 94 GHz constant width slot antennas (CSWA) on synthesized low dielectric constant substrates ($\epsilon_r = 2.2$). The performance of tapered slot antennas is sensitive to the effective thickness of the substrate. We have reduced the effective thickness by selectively machining holes in the dielectric substrate. The machined substrate antenna radiation patterns were significantly improved independent of the machined hole size or lattice as long as the quasi-static effective thickness remained the same, even if the hole/lattice geometry is comparable to a wavelength. The method was applied at 94 GHz on a constant width slot antenna with excellent radiation pattern improvement, making it suitable for f/1.6 imaging array applications.**

Keywords—**micromachining, artificial substrates, tapered slot antennas.**

I. Introduction

Tapered Slot Antennas (TSA) have been developed by Gibson et. al [1] and Yngvesson et. al [2], [3] for phased array and focal plane imagin systems. The performance of a TSA is sensitive to the thickness and dielectric constant of the antenna substrate. An *effective thickness*, which represents the electrical thickness of the substrate, has been defined as $t_{eff} = t(\sqrt{\epsilon_r} - 1)$. One accepted range of the effective thickness (determined experimentally) for good operation of a TSA is given as $0.005\lambda_o \leq t_{eff} \leq 0.03\lambda_o$ [2]. For substrate thickness above the upper bound of effective thickness, unwanted substrate modes develop which degrade the performance of the tapered slot antenna, while antennas on thinner substrates suffer from decreased directivity.

The upper bound on the effective thickness, $t_{eff} \leq 0.03\lambda_o$, necessitates mechanically thin substrates for mm-wave applications, even if low dielectric constant materials are used. For example, a maximum thickness of 200 μm (8 mils) is allowed for a 94 GHz TSA integrated on an $\epsilon_r = 2.2$ dielectric substrate. This results in a mechanically fragile substrate.

One way of improving the mechanical stability is to increase the thickness of the substrate and then selectively remove parts or nearly all of the underlying dielectric material. If nearly all of the substrate is removed, the TSA can be suspended on a thin dielectric membrane with an effective dielectric constant of $\epsilon_r = 1.05$ [4]. This is easily implemented at sub mm-wave frequencies (300 GHz-3 THz), but is not as practical at mm-wave frequencies (30-300 GHz) since the membrane dimensions are large and the mechanical stability of the suspended membrane is compromised. Other researchers (Vowinkel et al [5]) have selectively removed large portions of the dielectric inside the slot area of the TSA with good results.

Another method commonly used at mm-wave frequencies is the integration of the radiating antenna on a thin (4-8 mil) low dielectric substrate with $\epsilon_r = 2.2$ backed by a thick foam substrate with a dielectric constant of less than 1.1 [6], [7]. While this is excellent at 20-100 GHz, the thin dielectric substrate will interefere with the radiation patterns of Tapered Slot Antennas at frequencies greater than 100 GHz. Therefore, it is advantageous to develop a technique to further reduce the dielectric constant of the dielectric support substrate.

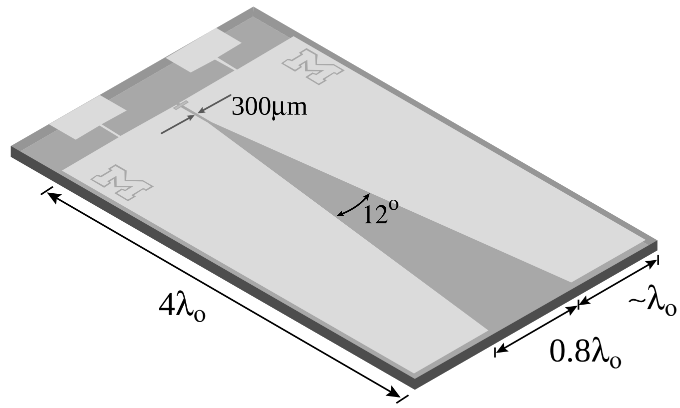

Fig. 1. The linear tapered slot antenna on a 1.27 mm thick RT/durioid ($\epsilon_r = 2.2$) substrate. The pads on the end of the antenna are for low frequency signal pickup.

In this work, an array of closely drilled holes is used to remove a portion of the underlying substrate, thereby resulting in a lower quasi-static (effective) dielectric constant substrate. This technique has been applied successfully using microstrip antennas [8]. The volume of the dielectric removed can be precisely controlled (between 0-100%) and determines the effective dielectric constant of the substrate. In this application, around 40-50% of the substrate is removed to maintain good mechanical properties.

II. 30 GHz Design & Measurements

A. LTSA Design

A non-optimal linear tapered slot antenna design, shown in figure 1, was chosen for the 30 GHz experiments. The LTSA was designed to be $4\lambda_o$ long with a 12° taper angle, which results in nearly one λ_o aperture. The slotline feed was 200-300 μm wide. The substrate is 1.27 mm (50 mils) thick RT/duriod, with a relative dielectric constant of $\epsilon_r = 2.2$. Three different substrates were investigated: *solid substrate*, *big hole substrate*, and *small hole substrate*. The big hole and small hole patterns, shown in figure 2, were machined in a 45-degree

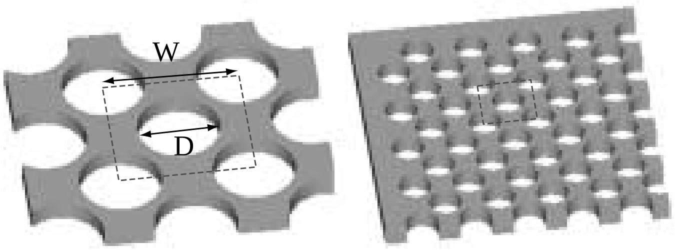

Fig. 2. Hole patterns machined into the substrates of the 30 GHz tapered slot antennas. The larger pattern has a hole diameter, D, of 3.18 mm (125 mils), and a spacing, W, of 5.08 mm (200 mils). The smaller pattern has a hole diameter of 1.27 mm (50 mils), and a spacing of 2.03 mm (80 mils). The dashed box represents the unit cell.

rotated rectangular lattice with an automated milling machine. The big hole substrate was chosen to be a large fraction of a wavelength with $D = \lambda_o/3$ (3.18 mm) and $W = \lambda_o/2$ (5.08 mm). The small hole pattern was chosen with $D = \lambda_o/8$ (1.27 mm) and $D = \lambda_o/5$ (2.03 mm). Previous measurements at 10 and 30 GHz have shown that the lattice choice (rectangular, hexagonal, etc.) has no effect on the far field patterns for low dielectric constant substrates [9].

The machined substrates were chosen to have the same effective relative dielectric constant. The effective dielectric constant is a quasi-static value, given by the volumetric average dielectric constant of the machined substrate, and is: $\epsilon_{eff} = \frac{\pi}{2}(\frac{D}{W})^2 + \epsilon_r[1 - \frac{\pi}{2}(\frac{D}{W})^2]$, where D and W are defined in figure 2.

For RT/duroid, with $\epsilon_r = 2.2$, the effective dielectric constant, ϵ_{eff}, is equal to 1.46 for the two machined substrates shown in figure 2. For a 30 GHz TSA integrated on 1.27 mm (50 mils) thick substrate, this reduction in the effective dielectric constant changes the value of t_{eff}/λ_o from 0.061 for the solid substrate to 0.026 for the machined substrates, placing the effective thickness just within the performance limits of Yngveson et al [2].

B. 30 GHz Measurements

The normalized radiation patterns of the antennas were measured in an anechoic chamber. The thin leads and the pads on the slot end of the antenna (Fig. 1) were designed to allow pickup of low frequency signals from a zero-bias Schottky diode (Metelics MSS20141-B10D, C_t = 0.8 pF) placed over the slot line of the antenna, one quarter of a guided wavelength from a capacitive RF short. The RF source was AM modulated at 5 kHz and radiated by a standard gain horn. The detected low frequency signal (5 kHz) at the diode terminals was delivered to a lock-in amplifier. The amplified signal was then read by a computer, which controled the antenna mount positioner.

The 30 GHz far field radiation patterns of the solid substrate and the big hole substrate antennas are shown in figure 3. There was significant improvement in the far field patterns of both the E- and H-plane with the machined substrates. Note the lower cross-polarization levels in the E- and H-plane patterns for the machined big hole antenna. No directivity values are quoted since the 45-plane co- and cross-polarization patterns were not measured. The big hole and the small hole tapered slot antennas

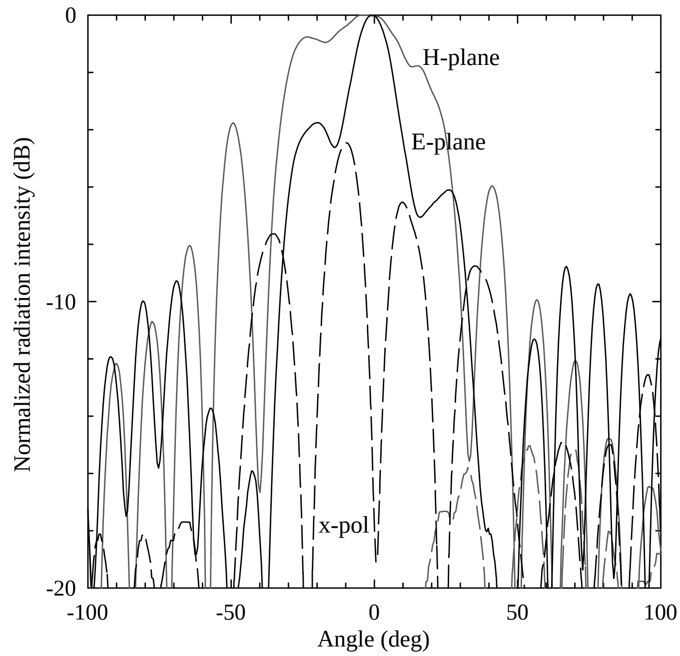

(a)

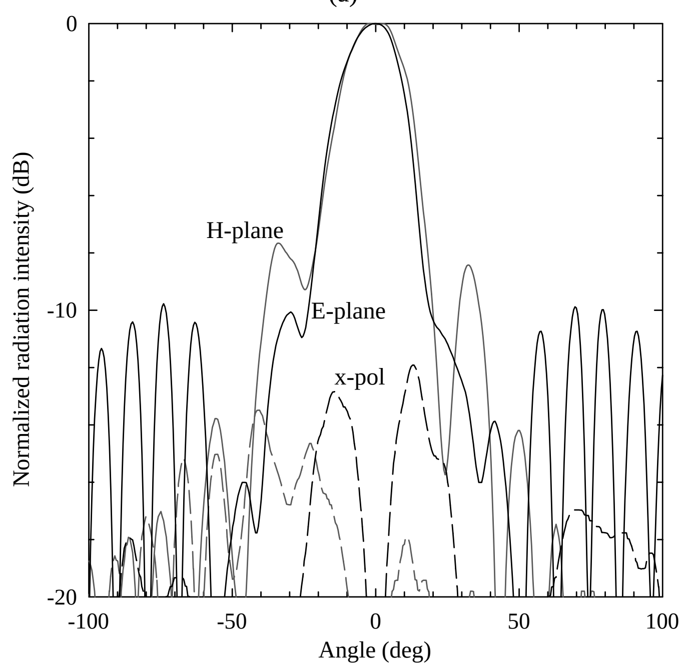

(b)

Fig. 3. Measured 30 GHz far field antenna patterns for the solid substrate (a) and the big hole LTSA(b).

TABLE I
COMPARISON OF THE 3-DB AND 10-DB BEAMWIDTHS FOR THREE DIFFERENT 30 GHZ TSA SUBSTRATES.

Antenna	3-dB		10-dB	
	E-plane	H-plane	E-plane	H-plane
Solid substrate	17	54	66	67
Big/small hole	25	26	42	43

gave very similar patterns to within $\pm 1^\circ$ and ± 1 dB (Fig. 4). This indicates that the improvement in performance is independent of hole geometry even if the holes/periods are a large fraction of a wavelength. This further suggests that the effect is purely a quasi-static reduction of the substrate dielectric constant, and not a mode suppression/photonic bandgap mechanism typically seen in high dielectric constant substrates [10].

The 3-dB and 10-dB beamwidths for all three antennas are summarized in Table I. Notice the fine structure (or ripple) in the measured patterns at angles above $\pm 40^\circ$. This is believed to be an interference pattern from the measurement setup and the edge of the TSA substrate. Recently, Sugawara et al. have shown that TSA patterns are very sensitive to currents induced on the edge of the finite-width substrate. These edge currents are in opposite phase to the slot-antenna currents and result in interference-like patterns at large measurement angles [11]. The big hole antenna results in symmetrical patterns at 30 GHz, and for a 10-dB taper in an imaging lens system, the antenna will fit an f/1.25 lens.

A comparison of the measured 24, 30, and 36 GHz far field radiation patterns for the big hole antenna is shown in figure 5. The backside radiation patterns ($|\theta| \geq 90^\circ$) were below -15 dB. The peak cross-polarization levels were below -12.5, -10.5, and -8.5 dB at 24, 30, and 36 GHz, respectively. The corresponding patterns of the small hole LTSA are virtually identical and are not shown. As the frequency increases, the beamwidth decreases, the side lobe levels increase, and the patterns degrade as the effective thickness increases (as expected). Note that even at 36 GHz with $D = \lambda_o/2.5$ and $W = \lambda_o/1.6$, the big hole TSA gave virtually identical patterns to the small hole TSA with $D = \lambda_o/6.3$ and $W = \lambda_o/4$.

III. 94 GHz DESIGN & MEASUREMENTS

A. 94 GHz Design

A constant width tapered slot antenna design, provided by Dr. Ellen Moore at Millimetrix Corporation, was used for the 94 GHz experiments (Fig. 6). In order to obtain an effective thickness of $t_{eff} \leq 0.03\lambda_o$ at 94 GHz, the solid substrate thickness must be less than 200 μm, resulting in a mechanically unstable substrate. Increasing the thickness to 380 μm (15 mils) improves the mechanical stability to a practical level. We compared 380 μm thick solid substrate antennas to antennas machined with a hole pattern, shown in figure 2, having a diameter of 380 μm ($\lambda_o/9$) and a spacing of 610 μm ($\lambda_o/5$). In retrospect, these dimensions were chosen to be unnecessarily small and can easily be enlarged by a factor or 2-3. The machining removes approximately 40% of the substrate and again results in an effective dielectric constant of 1.46. The effective thickness

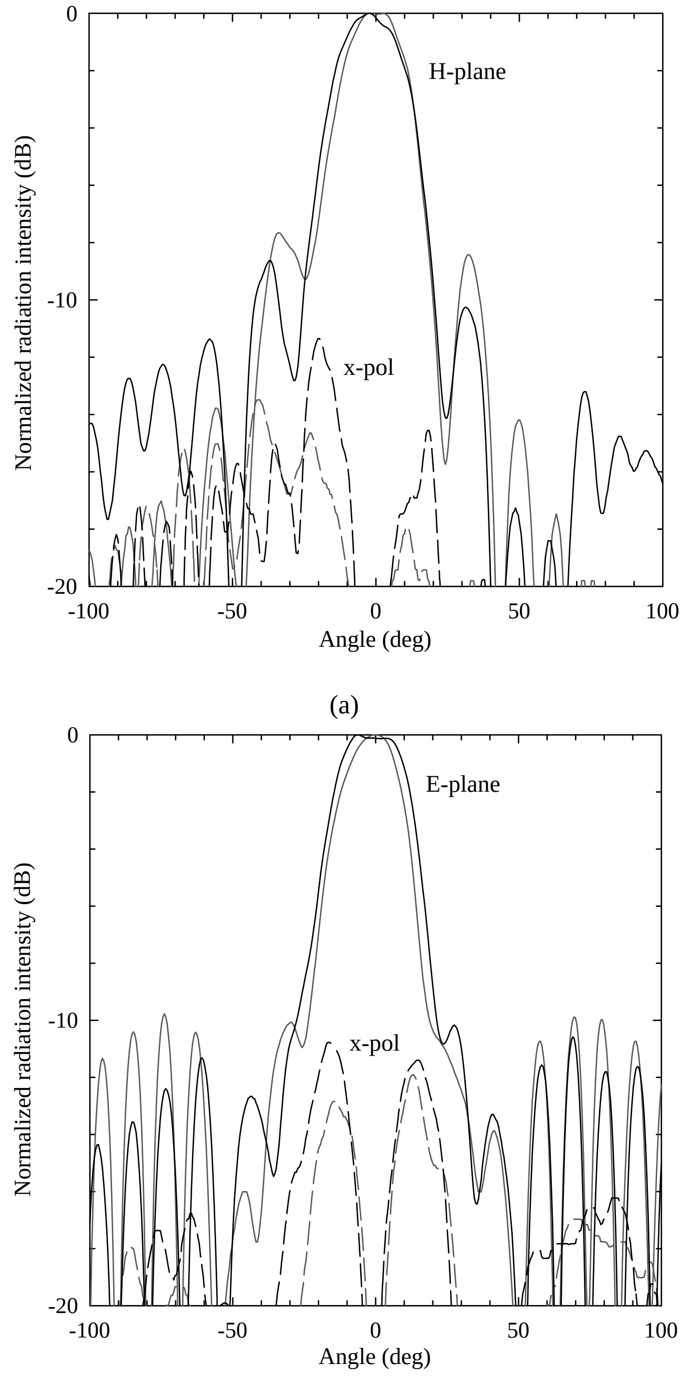

(b)

Fig. 4. Measured 30 GHz H-plane (a) and E-plane (b) far field antenna patterns for the big hole (gray) and small hole LTSA (black).

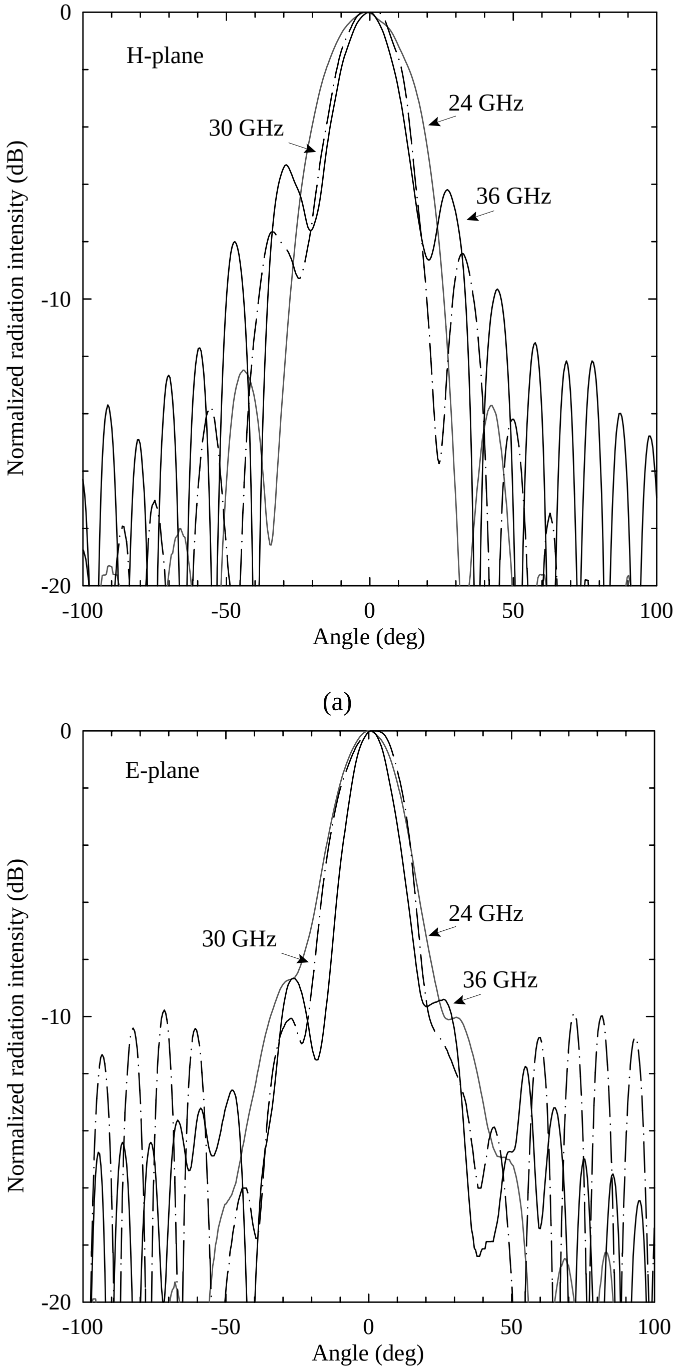

Fig. 5. Measured 24 (gray), 30 (dash-dot) and 36 GHz (solid) H-plane (a) and E-plane (b) far field co-polarization antenna patterns for the big hole LTSA.

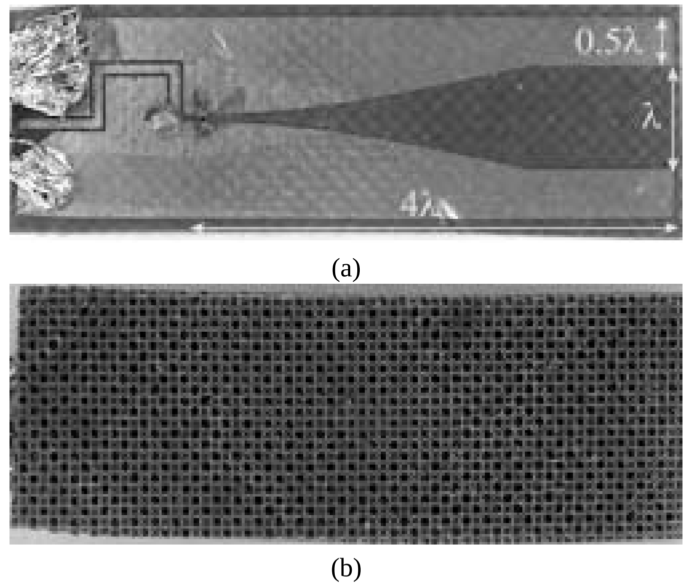

Fig. 6. Front-side conductor pattern (a) and back-side hole pattern (b) for the CWSA 94 GHz antenna. The antenna aperture is approximately λ_o, and the length is approximately $4\lambda_o$. The hole diameter is 380 μm and the unit cell width is 610 μm.

of the antenna is reduced from 0.058 to 0.025, again just within the acceptable limits.

B. 94 GHz Measurements

The 94 GHz measurements were performed on a bench top with absorber placed around the perimeter of the bench. The measurements were performed with an experimental setup similar to the 30 GHz setup, except with an AM modulated 94 GHz Gunn-diode source. An Alpha diode (DMK2784-000, C_t = 0.04 pF), placed across the slot, was used to detect the modulated signal. A signal to noise ratio of greater than 20 dB was achieved.

The 94 GHz far field antenna patterns for the solid substrate and the machined CWSA are shown in figure 7. The CWSA showed excellent pattern improvement for the machined case, with low cross polarization levels (-13 dB). The sharp -10 dB sidelobes are believed to be due to the edge currents on the finite width ($0.5\lambda_o$) conductor half plane. The machined CWSA results in an average -10 dB beamwidth of 35° and fits an f/1.6 lens imaging system. It is expected that the antenna patterns will change when placed in a 2-D imaging array, and this is subject to current investigation in our group.

IV. CONCLUSIONS

We have shown that selective machining of a thick dielectric substrate results in a simple method for reducing the effective thickness of tapered slot antennas. In contrast to earlier measurements on high-dielectric constant substrates, if low dielectric constant substrates are used, the improved far field radiation patterns are not sensitive to hole geometry or lattice choice (as long as the quasi-static effective thickness remains the same) and can be easily scaled with frequency from 10-94 GHz. A 94 GHz constant width tapered slot antenna on a thick machined

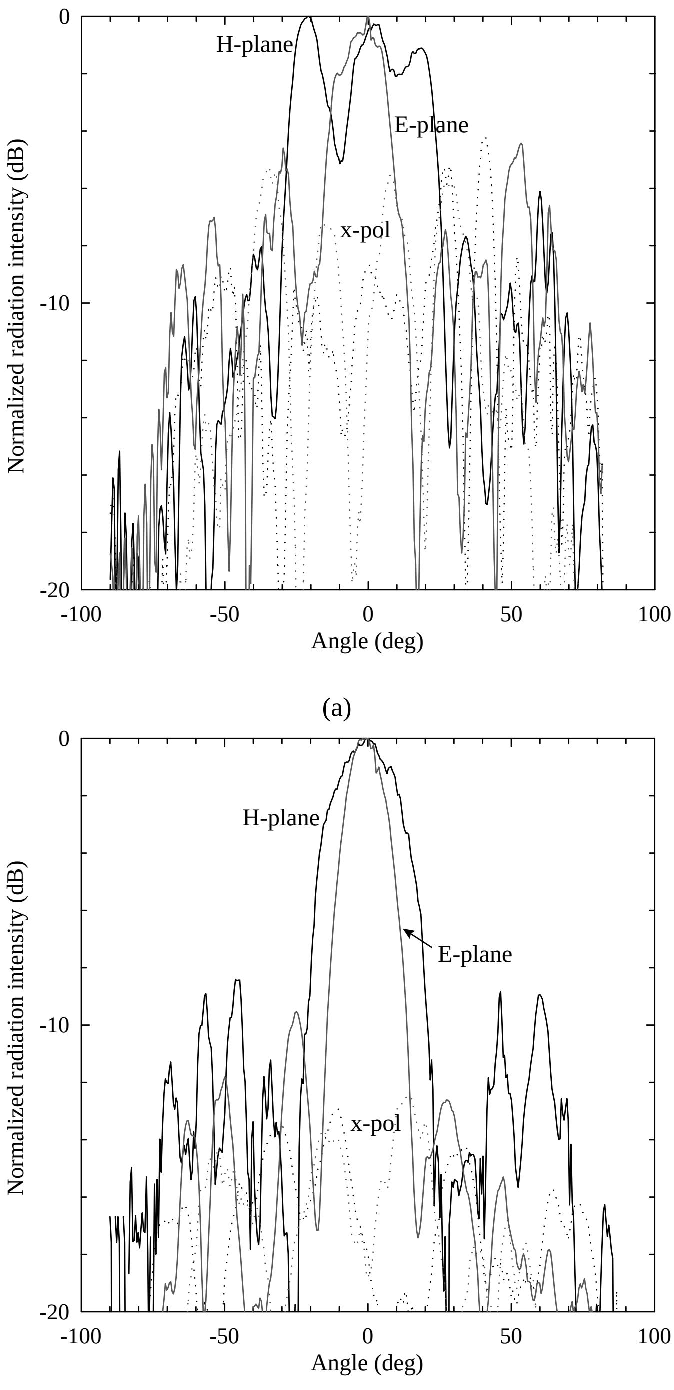

(a)

(b)

Fig. 7. Measured 94 GHz solid substrate (a) and machined substrate antenna (b) far field CSWA patterns.

substrate ($\epsilon_r = 2.2$) was successfully fabricated, showing mechanical stability and practical radiation performance, for imaging array applications.

REFERENCES

[1] P. J. Gibson, "The vivaldi aerial," in *Proc. 9th European Microwave Conference*, UK, June 1979, pp. 101–105.

[2] K. S. Yngvesson, "Endfire tapered slot antennas on dielectric substrates," *IEEE Transactions on Antennas and Propogation*, vol. 33, pp. 1392–1400, Dec 1985.

[3] K. S. Yngvesson, T. L. Koreniowski, Y. S. Kim, E. L. Kollberg, and J. F. Johansson, "The tapered slot antenna - a new integrated element for MM-wave applications," *IEEE Transactions on Antennas and Propogation*, vol. 37, pp. 365–374, Feb 1989.

[4] P. R. Acharya, H. Ekstrom, S. S. Gearhart, S. Jacobsson, J. F. Johansson, E. L. Kollberg, and G. M. Rebeiz, "The tapered slot antennas at 802 GHz," *IEEE Transactions on Microwave Theory and Techniques*, vol. 41, pp. 1715–1719, Oct 1993.

[5] U. K. Kotthaus and B. Vowinkel, "Investigation of planar antennas for submillimeter receivers," *IEEE Transactions on Microwave Theory and Techniques*, vol. 37, pp. 375–380, Feb 1989.

[6] J. F. Zürcher, "The SSFIP - a global concept for high performance braodband planar antennas," *Electronics Letters*, vol. 24, no. 23, pp. 1433–1435, November 1988.

[7] B. Zürcher, J. F. Zürcher, and F. Gardiol, "Braodband microstrip radiators: the SSFIP concept," *Electromagnetics*, vol. 9, pp. 385–393, November 1988.

[8] G. P. Gauthier, A. Courtay, and G. M. Rebiez, "Microstrip antennas on synthesized low dielectric-constant substrates," *IEEE Transactions on Antennas and Propogation*, vol. 45, pp. 1310–1314, Aug 1997.

[9] T. J. Ellis and G. M. Rebiez, "MM-Wave tapered slot antennas on micromachined photonic bandgap dielectrics," in *IEEE-MTT International Microwave Symposium*, San Francisco, CA, June 1996, pp. 1157–1160.

[10] T. J. Ellis and G. M. Rebiez, "Imporvements in tapered slot antennas on thick dielectric substrates," in *IEEE International Symposium on Antennas and Propagation*, Baltimore, MD, July 1996, pp. 992–995.

[11] S. Sugawara et al., "Characteristics of a MM-Wave tapered slot antenna with corrugated edges," in *IEEE-MTT International Symposium*, Baltimore, June 1998.